BBA - Molecular Basis of Disease 1870 (2024) 167192

Contents lists available at ScienceDirect

BBA - Molecular Basis of Disease

journal homepage: www.elsevier.com/locate/bbadis

Pan-neuronal expression of human mutant SOD1 in *Drosophila* impairs survival and motor performance, induces early neuroinflammation and chromosome aberrations

Francesco Liguori [a,b,*], Francesca Alberti [a,1], Susanna Amadio [a], Daniela Francesca Angelini [a], Eleonora Pilesi [c], Giuseppe Vitale [a,2], Giulia Tesoriere [c], Giovanna Borsellino [a], Fiammetta Vernì [c], Cinzia Volonté [a,b,*]

[a] *Experimental Neuroscience and Neurological Disease Models, IRCCS Fondazione Santa Lucia, Via del Fosso di Fiorano 65, 00143 Rome, Italy*
[b] *Institute for Systems Analysis and Computer Science "Antonio Ruberti" (IASI), National Research Council (CNR), Via dei Taurini 19, 00185 Rome, Italy*
[c] *Department of Biology and Biotechnology "Charles Darwin", Sapienza University of Rome, Piazzale Aldo Moro 5, 00185 Rome, Italy*

ARTICLE INFO

Keywords:
Drosophila
Amyotrophic lateral sclerosis
Neuroinflammation
Antimicrobial peptides
Chromosome aberrations

ABSTRACT

Several mutations in the *SOD1* gene encoding for the antioxidant enzyme Superoxide Dismutase 1, are associated with amyotrophic lateral sclerosis, a rare and devastating disease characterized by motor neuron degeneration and patients' death within 2–5 years from diagnosis. Motor neuron loss and related symptomatology manifest mostly in adult life and, to date, there is still a gap of knowledge on the precise cellular and molecular events preceding neurodegeneration.

To deepen our awareness of the early phases of the disease, we leveraged two *Drosophila melanogaster* models pan-neuronally expressing either the mutation A4V or G85R of the human gene *SOD1* (hSOD1^{A4V} or hSOD1^{G85R}).

We demonstrate that pan-neuronal expression of the hSOD1^{A4V} or hSOD1^{G85R} pathogenic construct impairs survival and motor performance in transgenic flies. Moreover, protein and transcript analysis on fly heads indicates that mutant hSOD1 induction stimulates the glial marker Repo, up-regulates the IMD/Toll immune pathways through antimicrobial peptides and interferes with oxidative metabolism. Finally, cytological analysis of larval brains demonstrates hSOD1-induced chromosome aberrations. Of note, these parameters are found modulated in a timeframe when neurodegeneration is not detected.

The novelty of our work is twofold: we have expressed for the first time *hSOD1* mutations in all neurons of *Drosophila* and confirmed some ALS-related pathological phenotypes in these flies, confirming the power of *SOD1* mutations in generating ALS-like phenotypes. Moreover, we have related SOD1 pathogenesis to chromosome aberrations and antimicrobial peptides up-regulation. These findings were unexplored in the SOD1-ALS field.

List of abbreviations

ALS	Amyotrophic Lateral Sclerosis
AMPs	Antimicrobial Peptides
C9ORF72	Chromosome 9 ORF 72
CCNF	Cyclin F
CNS	Central Nervous System
DCF	2′,7′-dichlorofluorescein
fALS	Familial Amyotrophic Lateral Sclerosis
FUS/TLS	Fused in Sarcoma/Translocated in Liposarcoma
Gst	Glutathione-S-Transferase
H_2DCF-DA	2′,7′-dichlorodihydrofluorescein diacetate
IMD	Immunodeficiency
ROS	Reactive Oxygen Species
sALS	Sporadic Amyotrophic Lateral Sclerosis
SOD1	Superoxide Dismutase 1

(*continued on next column*)

(*continued*)

(*continued on next page*)

* Corresponding authors at: Experimental Neuroscience and Neurological Disease Models, IRCCS Fondazione Santa Lucia, Via del Fosso di Fiorano 65, 00143 Rome, Italy.
E-mail addresses: f.liguori@hsantalucia.it (F. Liguori), cinzia.volonte@cnr.it (C. Volonté).
[1] Present address: TIGEM - Telethon Institute of Genetics and Medicine, Via Campi Flegrei 34, 80078 Pozzuoli (NA), Italy.
[2] Present address: Università Cattolica del Sacro Cuore and IRCCS Fondazione Policlinico Universitario Agostino Gemelli, Largo A. Gemelli 8, 00168 Rome, Italy.

https://doi.org/10.1016/j.bbadis.2024.167192
Received 1 November 2023; Received in revised form 4 April 2024; Accepted 15 April 2024
Available online 22 April 2024

(*continued*)

SOD2	Superoxide Dismutase 2
TARDBP	Tar DNA-Binding Protein
TDP-43	Tar DNA-Binding Protein 43

1. Introduction

Amyotrophic lateral sclerosis (ALS) is a rare and multifactorial neurodegenerative disease characterized by upper and lower motor neuron degeneration, causing impaired movement and respiratory failure, and leading to the death on average within 2–5 years from diagnosis [1,2]. The majority of ALS cases (90 %) is classified as sporadic (sALS), with no clear genetic linkage, while the remaining part (10 %) is defined as familial (fALS), with a distinct Mendelian inheritance [3,4]. Despite motor cortex and ventral horns of spinal cord being the mainly damaged CNS districts, ALS-related mutations are clearly inherited in all cells of the organism. More than 50 genes are associated with ALS [5]. *C9ORF72* (*Chromosome 9 ORF 72*, 40 % of cases), *SOD1* (*Superoxide Dismutase 1*, 12 %), *TARDBP* (*TAR DNA Binding Protein*, 4 %), *FUS/TLS* (*Fused in Sarcoma/Translocated in Liposarcoma*, 4 %), and *CCNF* (*Cyclin F*, 4 %) [2] are the most commonly reported as mutated and involved in more than half of fALS cases.

Mutations in *SOD1* were the first to be described as causative of the disease [6] and *SOD1* is the second most common ALS-associated gene [2], with >200 identified point mutations generally inherited as autosomal dominant [7,8], exception made for the D90A that shows an autosomal recessive pattern and is predominantly found in the Scandinavian population [9]. These mutations are distributed throughout the gene and impact on a variety of protein domains and functions.

The SOD1 protein is a ubiquitously expressed enzyme which converts the reactive superoxide anion into hydrogen peroxide, which in turn is processed by the catalase and peroxidase enzymes. Interestingly, recent evidence suggests new roles of SOD1 protein, both dependent and independent from enzymatic activity, thus corroborating the concept of the multifaceted aspect of this protein. Indeed, SOD1 acts as a signaling molecule to regulate cellular homeostasis, is involved in Treg cells differentiation and modulates intracellular calcium levels [10–13].

Since most of the mutant proteins retain their enzymatic function, pathogenicity is thought to be due to a combination of toxic loss- and gain-of-functions mediated and exacerbated by oxidative stress, hydrogen peroxide concentration shift, excitotoxicity, protein aggregation, neuroinflammation, apoptosis, mitochondrial dysfunction, deregulation of axonal transport, and endoplasmic reticulum stress [14–20].

Despite the huge effort of researchers and the generation of many in vitro and in vivo models [21], our knowledge about the molecular initiators of the ALS cascade remains elusive. Neurodegeneration in ALS is sustained by several factors that overall generate a pathogenic cascade triggering irreversible neuronal death, when a certain still undefined threshold damage is exceeded. Starting from this assumption, in this work we decided to better define and characterize the earliest pathways that become deregulated in ALS. To this aim, we took advantage of two *Drosophila melanogaster* models carrying a transgene encoding for two particular mutant forms (hSOD1^{G85R} or hSOD1^{A4V}) of the human *SOD1* gene [22]. Specifically, the A4V (alanine to valine substitution at codon 4) mutation is related to >50 % of *SOD1* ALS-associated mutations in North America [23,24], while it is rare in Europe, probably due to population genetics phenomena, such as founder effect and migration [24]. Individuals carrying the A4V mutation can manifest ALS at any age, with a marked and sudden onset of symptoms and a very rapid progression of the disease, generally culminating to death after less than two years [25–27]. Concerning the G85R mutation (arginine replaced by glycine at codon 85), it is characterized by a rapid progression despite mutant SOD1 accumulates at very low levels. Mechanistically, SOD1-G85R proteins are defective in metal ions and consequently are not able to fulfill their role as antioxidant, also because this mutation is located near the active site [28].

We decided to express these transgenes in all neurons of *Drosophila*, which is a very well-established model where to dissect the molecular basis of ALS, not only because transgenic flies recapitulate many features of the disease, but also because they are valuable for screening possible beneficial therapeutic compounds, having a very short life cycle with very abundant progeny [29–31]. This adds to the availability of peculiar transgenesis programs that allow the direct expression of a transgene in a specific cell type of the fly, thus helping to precisely dissect the contribution of a distinct cell phenotype during disease progression. Leveraging these numerous potentialities and aiming to clarify the potential contribution of all neurons carrying the *SOD1* mutation to the pathogenesis, we demonstrated that pan-neuronal expression of hSOD1^{A4V} and hSOD1^{G85R} decreases survival rate and causes motor impairment compared to non-mutant controls. Moreover, it determines gliosis, innate immunity activation and antimicrobial peptides (AMPs) up-regulation, oxidative stress, and chromosome aberrations. These events occurred since the very early days of fly adult life, when ALS-induced neurodegeneration is not detected. Taken together, these results indicate that SOD1-ALS pathogenesis is characterized by a very precocious neuroinflammatory component that perhaps might trigger the progressive cascade of damage leading to the typical ALS pathology.

2. Material and methods

2.1. Drosophila strains

The *Drosophila* stocks used to carry out the experiments described in this manuscript have been purchased from Bloomington *Drosophila* Stock Center (Bloomington, IN, USA) and are:

- w^{1118}; P-w[+mC]=UAS-hSOD1.A4V-9.1/TM6B, Tb^{1} (BL33607)
- w^{1118}; P-w[+mC]=UAS-hSOD1.G85R-2a; 2b; 3a; 3b (BL33608)
- P-w[+mW.hs]=GawB-elav[C155] (BL458)
- w*; P-w[+mC]=GAL4-ninaE.GMR-12 (BL1104)
- w^{1118}; P-y[+t7.7]-w[+mC]=UAS-GGGGCC.36}attP40 (BL58688)

All experiments were normalized or compared with non-mutant control elav-Gal4/+ flies, obtained crossing elav-Gal4 flies with the OregonR wild-type strain. We do not used as control flies pan-neuronally expressing human wild-type SOD1, because its expression is reported to be toxic per se [22]. It is indeed well-known that the overexpression of a wild-type gene product can cause mutant phenotypes likewise mutant ones [32]. Flies expressing human FUS^{R518K} transgene [33] were kindly provided by Professor Udai Pandey (University of Pittsburgh, PA, USA). Flies expressing elav-driven UAS-mCD8:GFP transgene (P-w[+mW.hs]=GawB-elav[C155], P-w[+mC]=UAS-mCD8-GFP.L-Ptp4E[LL4], P-ry[+t7.2]=hsFLP, BL5146) were a kind gift of Professor Lucia Piacentini (Sapienza University of Rome, Italy). Stocks were maintained at 25 °C, in a 12:12 light/dark cycle and fed with standard sugar-cornmeal-yeast-agar nutritional medium, supplemented with propionic acid (cat. 409553, Carlo Erba Reagents, Cornaredo, Italy) as powerful mold inhibitor. All genetic crosses were performed at 25 °C.

2.2. Lifespan assay

Lifespan was measured according to [34]. Briefly, for each experimental group, flies (n = 134–180) were subdivided into vials with 20 flies each. Every two days, flies were transferred to new vials and dead flies were scored. Escaped or accidentally lost flies were considered right-censored and not included in the curves. Survival curves were analyzed by log-rank method with Bonferroni correction through OASIS 2 (Online Application for the Survival Analysis) online software [35].

2.3. Climbing assay

Climbing assay was performed according to [36]. For each experimental group, flies ($n = 100$) were subdivided into vials with 10 flies each. At specific timepoints (0–3-, 9–12-, 17–20-, 25–28-, 33–36-, 41–44- and 49–52-days post-eclosion), flies were placed into a closed vial (in the absence of nutritional medium) with a line drawn at 8 cm from the base. Vials were then tapped down in order to let flies fall to the bottom and stimulate their negative geotaxic reflex. Flies reaching the marked line within 10 s (goal-reaching flies) were counted. Each vial was tested three times. The mean value of total tested flies and the mean value ± SEM of goal-reaching flies were evaluated and reported in graph. To prevent differences due to circadian rhythm, climbing tests were always performed at the same time of the day. Statistical significance was evaluated with 2-way-ANOVA test with Dunnett's multiple comparisons correction.

2.4. Drosophila eye imaging

Flies were ether-anesthetized and eye pictures acquired through a stereomicroscope equipped with image acquisition system (Bio Cell, Rome, Italy). Pictures were further processed with Adobe Photoshop (Adobe, USA).

2.5. Western blot

To obtain total protein extracts, 10 fly heads were homogenized in SDS-Sample Buffer (50 mM TrisHCl pH 6.8, 2 % SDS, 100 mM dithiothreitol, 2.5 % glycerol, 0.1 % bromophenol blue) and heated at 85 °C for 8 min. Protein extracts were separated by 10 % SDS-PAGE and transferred onto nitrocellulose membrane (Protran, Merck, Darmstadt, Germany) in 20 % ethanol in Tris-Glycine buffer. Membranes were blocked for 30 min in 5 % non-fat dry milk TBS-T solution (10 mM Tris pH 8, 150 mM NaCl, 0.1 % Tween 20) and then incubated over-night at 4 °C with the specified primary antibodies. Membranes were next incubated with HRP-conjugated anti-rabbit or anti-mouse secondary antisera (1:5000 diluted in 5 % non-fat dry milk TBS-T buffer) for 1 h at room temperature. The conserved and ubiquitous Giotto protein, which plays a prominent role in the cytokinesis of neuroblasts [37,38], was used as loading control, as commonly adopted when analyzing fly neuronal protein extracts [39,40]. Immunostained bands were visualized using Super Signal West Pico Plus ECL (Thermo Scientific, Waltham, MA, USA) on iBright CL1000 Imaging System (Invitrogen, Waltham, MA, USA) and quantified using Image J software.

The primary antisera were:

- mouse anti-Elav, 1:500, 9F8A9 (Developmental Studies Hybridoma Bank, DSHB, Iowa, IA, USA)
- mouse anti-Repo, 1:500, 8D12 (DSHB)
- rabbit anti-Cu/Zn-SOD1, 1:2000, ADI-SOD-101 (Enzo Life Sciences, Farmingdale, NY, USA)
- rabbit anti-Giotto, 1:10000, [37].

2.6. Immunofluorescent staining of Drosophila adult brain

Immunofluorescence on adult fly brain was performed as previously described in [41] with slight modifications. Briefly, brains were dissected in PBS and fixed for 30 min on a rotating wheel in a 4 % formaldehyde PBS solution. After 3 washes in a PBST solution (PBS, 0.2 % Triton), blocking was performed for 50 min in 5 % NDS (Normal Donkey Serum, Merck) PBST solution. Mouse anti-Repo and rabbit anti-hSOD1 primary antibodies (1:200) were diluted in 1 % NDS PBST solution and incubated over two nights at 4 °C on a rotating wheel. After 3 washes in PBST, samples were incubated over two nights at 4 °C with fluorescent-labeled secondary antibodies (donkey anti-mouse Alexa Fluor 555-conjugated and donkey anti-rabbit Alexa Fluor 647-conjugated, 1:300 in 1 % NDS PBST) and then stained with DAPI to visualize nuclei. Brains were then mounted in Fluoromount medium (Merck) onto microscope slides. Immunofluorescence analysis was performed by confocal laser scanning microscope (LSM800, Zeiss) equipped with four laser lines: 405 nm, 488 nm, 561 nm, and 639 nm. The brightness and contrast of the digital images were adjusted using Zeiss Zen software 3.0 blue edition (Zeiss) and Adobe Photoshop (Adobe, USA).

2.7. Total RNA extraction, reverse transcription and qPCR

For each genotype, 30 adult heads were collected at specific timepoints and stored in RNA later (Merck) at −20 °C. Total RNA was isolated by Qiazol lysis reagent (Qiagen, Hilden, Germany) according to the manufacturer's instructions. After genomic DNA elimination, reverse transcription was achieved using PrimeScript RT Reagent Kit with gDNA Eraser (Takara Bio, Kyoto, Japan). qPCR reactions were carried out with TB Green® Premix Ex Taq™ (Takara Bio) and relative quantification of the transcripts was determined using the comparative Ct method, with *rp49* or *actin* genes as endogenous control. The normalization process was performed according to the formulae ΔCt = Ct value of transcript of interest - Ct value of the endogenous transcript. All experiments were performed in at least three independent biological replicates and each with three technical replicates. Used primers are:

Gene target	Oligonucleotide
Dm_Actin_F	GCTTCGCTGTCTACTTTCCA
Dm_Actin_R	CAGCCCGACTACTGCTTAGA
Dm_Attacin_F	GGGCTACAACAATCATGGA
Dm_Attacin_R	GACCTTTGATGTGGGAGTAG
Dm_Catalase_F	CAACCCCTTCGATGTCACCA
Dm_Catalase_R	TCTGCTCCACCTCAGCAAAG
Dm_Cecropin_F	AAGCTGGGTGGCTGAAGAAA
Dm_Cecropin_R	TGTTGAGCGATTCCCAGTCC
Dm_Defensin_F	CGTGGCTATCGCTTTTGCTC
Dm_Defensin_R	TTTGAACCCCTTGGCAATGC
Dm_Diptericin_R	ATCCTTGCTTTGGGCTTC
Dm_Diptericin_F	CCTGAACCACTGGCATAT
Dm_Drosocin_F	TTTTCCTGCTGCTTGCTTGC
Dm_Drosocin_R	GGCAGCTTGAGTCAGGTGAT
Dm_Drosomycin_F	CTGGGACAACGAGACCTGTC
Dm_Drosomycin_R	ATCCTTCGCACCAGCACTTC
Dm_GstD1_F	CGCGCCATCCAGGTGTATTT
Dm_GstD1_R	CTGGTACAGCGTTCCCATGT
Dm_Metchnikowin_F	GCTACATCAGTGCTGGCAGA
Dm_Metchnikowin_R	TTAGGATTGAAGGGCGACGG
Dm_rp49_F	GCGCACCAAGCACTTCATC
Dm_rp49_R	TTGGGCTTGCGCCATT
Dm_Sod1_F	GCACTTCAATCCGTATGGCAA
Dm_Sod1_R	CGAAGAGCGTAATCTTGGAGTC
Dm_Sod2_F	CAAACTGCAAGCCTGGCG
Dm_Sod2_R	CTGGTGGTGCTTCTGGTGAT

2.8. Total ROS measurements

Reactive Oxygen Species (ROS) measurement was performed as reported [42] with some modifications. Briefly, 50 fly heads were isolated and incubated in 0.5 % Trypsin-EDTA solution for 1 h at 37 °C, to obtain a single cell suspension. Cells were filtered on a 70 μm strainer to remove debris or undigested tissue and then centrifuged for 10 min at 5000 rpm. Pellets were resuspended and incubated in the dark at 37 °C for 30 min in PBS containing 10 μM 2′,7′-dichlorodihydrofluorescein diacetate (H_2DCF-DA; Molecular Probes, Carlsbad, CA, USA) dye. After centrifugation at 1840 ×*g* for 10 min, pellets were resuspended in PBS and then analyzed by flow cytometry using CytoFLEX (Beckman Coulter, Brea, CA, USA) to detect the fluorescent intensity of the 2′,7′-dichlorofluorescein (DCF) dye, indicative of ROS-positive cells. For each sample, approximately 20000 events were selected based on scatter parameters and the analysis was conducted after the exclusion of coincident events.

2.9. Mitotic chromosome preparations

Colchicine-treated larval brains were obtained for metaphase chromosome aberration scoring as described [43]. Fixed preparations were mounted in Vectashield H-1200 with DAPI (Vector Laboratories, Newark, CA, USA) to stain the DNA. Cytological preparations were examined with a Carl Zeiss Axioplan fluorescence microscope, equipped with an HBO100W mercury lamp and a cooled charged-coupled device (CCD camera; Photometrics CoolSnap HQ). At least 500 cells for condition were scored from 5 to 10 brains.

2.10. Key resources table

Reagent or resource	Source	Identifier
Antibodies		
Alexa Fluor 555-conjugated donkey anti-mouse	Thermo Fisher Scientific	Cat: #A32773 RRID: AB_2762848
Alexa Fluor 647-conjugated donkey anti-rabbit	Thermo Fisher Scientific	Cat: #A32795 RRID: AB_2762835
HRP-conjugated anti-mouse IgG secondary antibody	Thermo Fisher Scientific	Cat: #31430 RRID: AB_228307
HRP-conjugated anti-rabbit IgG secondary antibody	Thermo Fisher Scientific	Cat: #31460 RRID: AB_228341
Mouse monoclonal anti-Elav 9F8A9	Developmental Studies Hybridoma Bank	Cat: #ELAV 9F8A9, RRID: AB_2314364
Mouse monoclonal anti-Repo 8D12	Developmental Studies Hybridoma Bank	Cat: #8D12 RRID: AB_528448
Rabbit monoclonal anti-Cu/Zn SOD1	Enzo Life Sciences	Cat: #MAB0684 RRID: AB_1533264
Rabbit polyclonal anti-Giotto	[37]	RRID: AB_2892585
Chemicals, peptides, and recombinant proteins		
DAPI	Sigma-Aldrich	Cat: #D4592 CAS: 28718-90-3
H2DCF-DA	Molecular Probes	Cat: #D399
Critical commercial assays		
PrimeScript RT Reagent Kit with gDNA Eraser	Takara Bio	Cat: #RR047B
TB Green® Premix ExTaq™	Takara Bio	Cat: #RR42WR
Experimental models: organisms/strains		
D. melanogaster: Overexpression of human SOD1 with A4V mutation under UAS control: w1118; Pw[+mC] = UAS-hSOD1.A4V-9.1/TM6B, Tb1	Bloomington Drosophila Stock Center	RRID: BDSC_33607 FlyBase: FBst0033607
D. melanogaster: Overexpression of human SOD1 with G85R mutation under UAS control: w1118; Pw[+mC] = UAS-hSOD1.G85R-2a; 2b; 3a; 3b	Bloomington Drosophila Stock Center	RRID: BDSC_33608 FlyBase: FBst0033608
D. melanogaster: Overexpression of RNA and protein from 36 'pure' repeats of 'GGGGCC' under UAS control: w1118; P-y[+t7.7]-w[+mC] = UAS-GGGGCC.36}attP40	Bloomington Drosophila Stock Center	RRID: BDSC_58688 FlyBase: FBst0058688
D. melanogaster: Co-expresses CD8-tagged GFP under the control of UAS and GAL4 in neurons under elav control: Pw[+mW.hs] = GawB-elav[C155], Pw[+mC] = UAS-mCD8-GFP.L-Ptp4E[LL4], P-ry[+t7.2] = hsFLP	Bloomington Drosophila Stock Center	RRID: BDSC_5146 FlyBase: FBst0005146
D. melanogaster: Overexpression of human FUS with R518K mutation under UAS control	[33]	N/A
D. melanogaster: Expresses GAL4 in neurons under elav control: P{w[+mW.hs] = GawB}elav[C155]	Bloomington Drosophila Stock Center	RRID: BDSC_458 FlyBase: FBst0000458
D. melanogaster: Expresses GAL4 in the eye under GMR control: w[*]; P{w[+mC] = GAL4-ninaE.GMR}12	Bloomington Drosophila Stock Center	RRID: BDSC_1104 FlyBase: FBst0001104
Oligonucleotides		
Primers for qRT-PCR: See Material and methods section	This paper	N/A
Software and algorithms		
Adobe Photoshop CS6	Adobe	https://www.adobe.com/products/photoshop.html
ZEN Software	Zeiss	https://www.zeiss.com/microscopy/int/products/microscope-software/zen-lite.html

3. Results

3.1. $hSOD1^{A4V}$ and $hSOD1^{G85R}$ mutations impact on fly survival and motor performance

In order to dissect the early pathways that are deregulated in ALS we exploited two *Drosophila* models expressing the mutant $hSOD1^{G85R}$ or $hSOD1^{A4V}$ form of the human *SOD1* gene in all neurons, by using the well-known bipartite system Gal4-UAS [44]. In particular, transgene pan-neuronal expression was achieved through the elav-Gal4 driver [45]. Once verified the effective induction of human SOD1 by Western blot (Fig. 1A), we characterized the suitability of these models for ALS by firstly measuring lifespan. Flies carrying $hSOD1^{A4V}$ or $hSOD1^{G85R}$ transgene in all neurons (elav-Gal4 > UAS-$hSOD1^{A4V}$ or elav-Gal4 > UAS-$hSOD1^{G85R}$) displayed reduced survival rates compared to non-mutant controls (elav-Gal4/+) (Fig. 1B). In particular, while control flies lived 79 days (median lifespan of 54.29 ± 1.21 days), we registered a reduction in survival days of 19 % for A4V flies (64 days, with a median lifespan of 39.6 ± 1.22 days corresponding to 27 % reduction respect to controls) and of 7.5 % for G85R flies (73 days, with a median lifespan of 47.69 ± 1.03 days corresponding to 12 % reduction respect to controls). Moreover, the estimated time at 50 % survival was 56 days for elav-Gal4/+, 42 days for elav-Gal4 > UAS-$hSOD1^{A4V}$ and 49 days for elav-Gal4 > UAS-$hSOD1^{G85R}$ (Fig. 1B).

To further validate our models, we next investigated the motor ability by evaluating the negative geotaxic reflex of elav-Gal4 > UAS-$hSOD1^{A4V}$ and elav-Gal4 > UAS-$hSOD1^{G85R}$ flies at different time-points. Our results show that both mutations similarly impair motor performance by about 20 % already at 0–3 days and about 50 % at 17–20 days post-eclosion, as measured by climbing ability compared with age-matched non-mutant controls. With advancing ageing, the differences between control and mutant flies attenuate (Fig. 1C).

3.2. $hSOD1^{A4V}$ and $hSOD1^{G85R}$ expression does not promote neurodegeneration but stimulates gliosis

Considering that the *Drosophila* eye is an optimal tissue for the study of the genetic control of neurodegeneration [39,46], and that eye-specific expression of human ALS proteins such as FUS and C9ORF72 determines an aberrant eye conformation (Supplementary File 1)

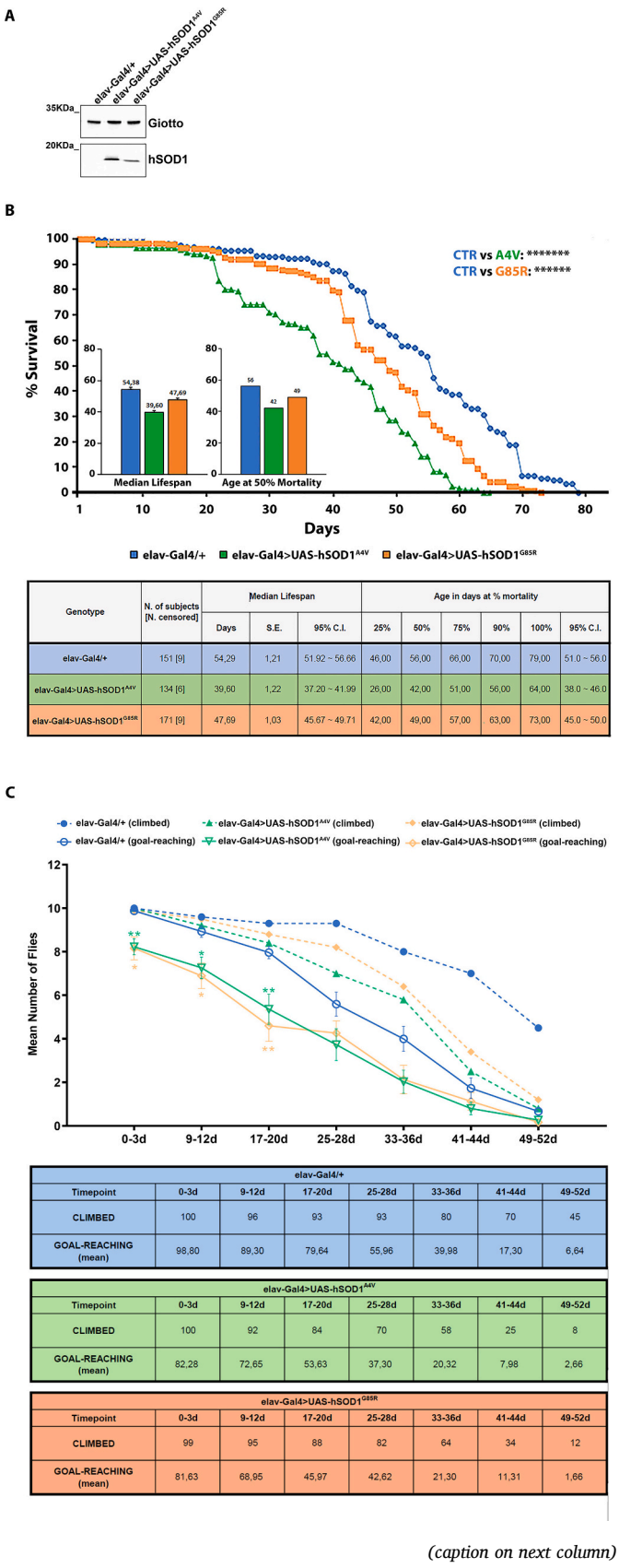

Genotype	N. of subjects [N. censored]	Median Lifespan			Age in days at % mortality					
		Days	S.E.	95% C.I.	25%	50%	75%	90%	100%	95% C.I.
elav-Gal4/+	151 [9]	54,29	1,21	51.92 ~ 56.66	46,00	56,00	66,00	70,00	79,00	51.0 ~ 56.0
elav-Gal4>UAS-hSOD1A4V	134 [6]	39,60	1,22	37.20 ~ 41.99	26,00	42,00	51,00	56,00	64,00	38.0 ~ 46.0
elav-Gal4>UAS-hSOD1G85R	171 [9]	47,69	1,03	45.67 ~ 49.71	42,00	49,00	57,00	63,00	73,00	45.0 ~ 50.0

elav-Gal4/+							
Timepoint	0-3d	9-12d	17-20d	25-28d	33-36d	41-44d	49-52d
CLIMBED	100	96	93	93	80	70	45
GOAL-REACHING (mean)	98,80	89,30	79,64	55,96	39,98	17,30	6,64

elav-Gal4>UAS-hSOD1A4V							
Timepoint	0-3d	9-12d	17-20d	25-28d	33-36d	41-44d	49-52d
CLIMBED	100	92	84	70	58	25	8
GOAL-REACHING (mean)	82,28	72,65	53,63	37,30	20,32	7,98	2,66

elav-Gal4>UAS-hSOD1G85R							
Timepoint	0-3d	9-12d	17-20d	25-28d	33-36d	41-44d	49-52d
CLIMBED	99	95	88	82	64	34	12
GOAL-REACHING (mean)	81,63	68,95	45,97	42,62	21,30	11,31	1,66

(caption on next column)

Fig. 1. Pan-neuronal expression of hSOD1^{A4V} and hSOD1^{G85R} ALS constructs reduces lifespan and impairs locomotor abilities. A) Western blot analysis of hSOD1 expression in non-mutant (elav-Gal4/+) and ALS (elav-Gal4 > UAS-hSOD1^{A4V} and elav-Gal4 > UAS-hSOD1^{G85R}) fly heads. The conserved and ubiquitous protein Giotto was used as loading control. B) Survival curves were obtained assaying elav-Gal4/+ (blue line, $n = 151$), elav-Gal4 > UAS-hSOD1^{A4V} (green line, $n = 134$) and elav-Gal4 > UAS-hSOD1^{G85R} (orange line, $n = 171$) flies. Inset bar graphs show the difference in terms of median lifespan and age at 50 % survival. Statistical significance was calculated by log-rank test with Bonferroni correction; elav-Gal4/+ vs elav-Gal4 > UAS-hSOD1^{A4V}: $p = 0.0000001$, elav-Gal4/+ vs elav-Gal4 > UAS-hSOD1^{G85R}: $p = 0.0000001$. The inset table resumes the number of analyzed subjects, the median lifespan ± S.E. (with the confidence interval at 95 %, 95% C.I.) and the fly age (in days) at 25 %, 50 %, 75 %, 90 % and 100 % mortality for each genotype (with 95 % C.I.). C) Non-mutant (elav-Gal4/+, blue lines) and ALS flies (elav-Gal4 > UAS-hSOD1^{A4V} – green lines and elav-Gal4 > UAS-hSOD1^{G85R} – orange lines) were assayed for climbing activity at different time-points (0–3, 9–12, 17–20, 25–28, 33–36, 41–44 and 49–52-days post-eclosion) measuring their negative geotaxis reflex. Flies reaching the marked line within 10 s (goal-reaching flies – continuous lines with empty symbols) were counted. Each vial was tested three times. The mean value of total tested flies (dotted lines with full symbols) and the mean value ± SEM of goal-reaching flies are reported in graph. The inset tables report the total number of tested and goal-reaching flies for each experimental group. Statistical significance was calculated by 2-way-ANOVA test with Dunnett's multiple comparisons correction. $^{*}p < 0.05$, $^{**}p < 0.01$.

[33,47,48], we investigated if also the expression of mutant hSOD1 had an effect on eye neurodegeneration and gross ommatidial morphology and pigmentation. To do so, we crossed UAS-hSOD1^{G85R} or UAS-hSOD1^{A4V} flies with those carrying the eye-specific driver GMR-Gal4 [49] and tested the effective induction of human mutant SOD1 by Western blot (Fig. 2A). As shown in Fig. 2B, the measured parameters are totally preserved compared to control eyes (GMR-Gal4/+) in adult flies both at 0–3 and 17–20 days post-eclosion, thus indicating absence of neurodegeneration.

To further confirm that the induction of the ALS transgenes in this early timeframe did not induce neuronal depletion, we performed Western blot analysis on pan-neuronally-expressing-hSOD1-fly heads at 0–3 and 17–20 days. As a global indicator of neuronal content, we adopted the neuronal marker Elav, which has a role in axon guidance and synapse formation. Fig. 2C shows that pan-neuronal expression of hSOD1^{A4V} or hSOD1^{G85R} does not decrease Elav protein expression at both 0–3 days and 17–20 days. However, as expected, we also observed a significant age-related neuronal depletion in both healthy (elav-Gal4/+) and ALS flies. This result indicates the absence of neurodegeneration in the first twenty days of elav-Gal4 > UAS-hSOD1^{A4V} and elav-Gal4 > UAS-hSOD1^{G85R} fly life.

With the aim to investigate if and how ectopic expression of human ALS transgene impacts on glia [50,51], we then evaluated the expression of the glia marker Repo, a homeodomain transcription factor specifically expressed in glial cells and required for acquisition of glial fate and subsequent terminal differentiation. Our results show that Repo levels, contrarily to Elav, are significantly and transiently up-regulated only in 0–3 days old hSOD1^{A4V} and hSOD1^{G85R} flies respect to healthy samples, as shown by Western blot (Fig. 2C). To better define Repo expression pattern in response to mutant hSOD1 overexpression (Fig. 2D, panels *d* and *h*) and contemporarily assess the absence of neurodegeneration, we performed a double immunofluorescent staining against Repo and hSOD1 proteins on 0–3 days adult brains pan-neuronally expressing membrane-tethered GFP (UAS-mCD8:GFP, to highlight Elav expression pattern) and hSOD1^{A4V} or hSOD1^{G85R} constructs. Confocal microscopy images confirm that hSOD1 transgenic samples (elav-Gal4 > UAS-mCD8:GFP; UAS-hSOD1^{A4V} or elav-Gal4 > UAS-mCD8:GFP; UAS-hSOD1^{G85R}) not only exhibit a high degree of Repo-positive foci spreading out in all districts of the brain (Fig. 2D, panels *a*, *e*, *i*), with

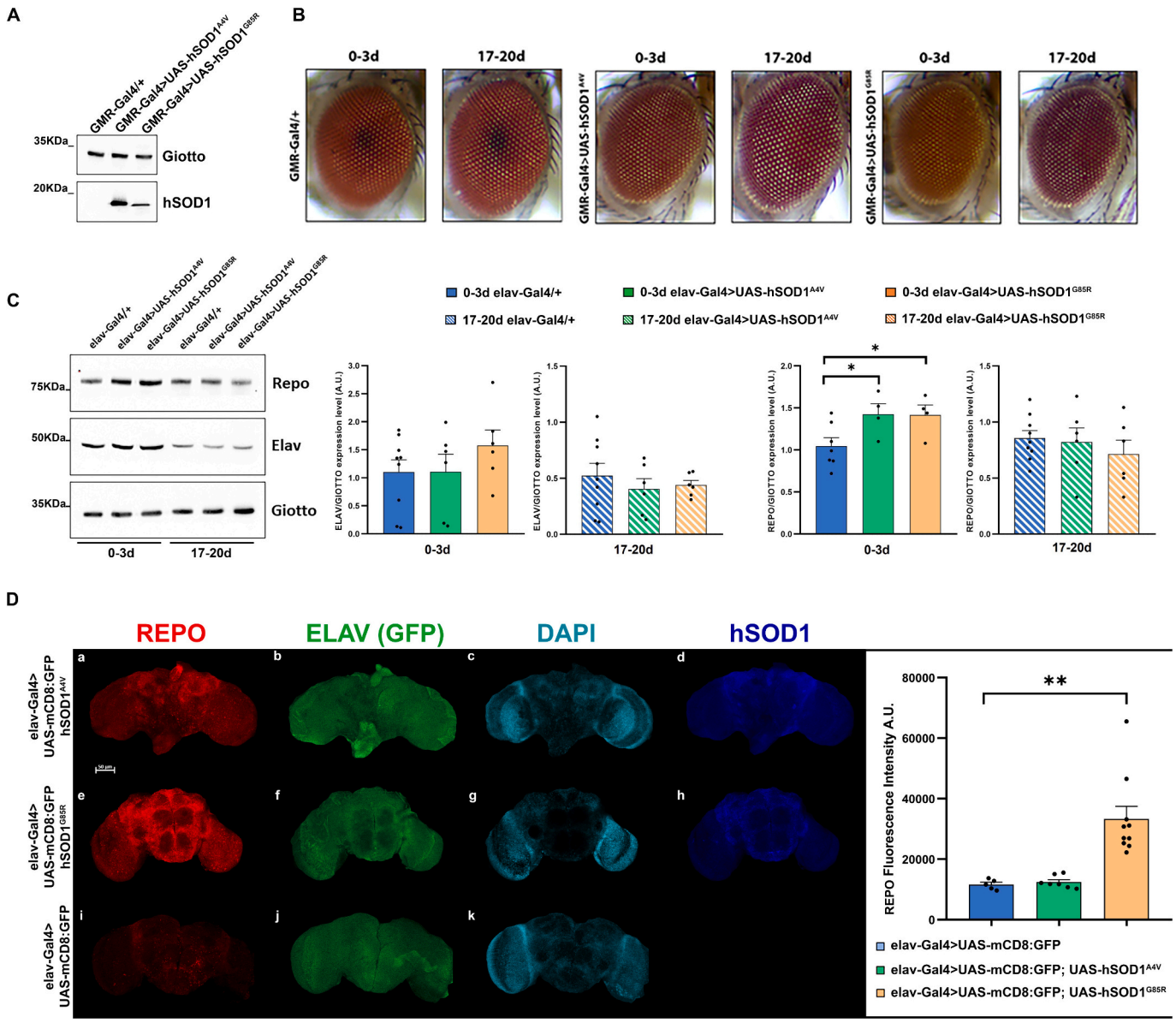

Fig. 2. Pan-neuronal expression of hSOD1^{A4V} and hSOD1^{G85R} ALS constructs promotes early gliosis but not neurodegeneration. A) Western blot analysis of hSOD1 expression in control (GMR-Gal4/+) and ALS (GMR-Gal4 > UAS-hSOD1^{A4V} and GMR-Gal4 > UAS-hSOD1^{G85R}) flies confirms the effective GMR-eye-specific induction of human *SOD1* transgene. The conserved and ubiquitous protein Giotto was used as loading control. B) Bright-field microscopy images from 0 to 3 days post-eclosion and 17–20 days post-eclosion control (GMR-Gal4/+) and ALS (GMR-Gal4 > UAS-hSOD1^{A4V} - GMR-Gal4 > UAS-hSOD1^{G85R}) fly eyes. The expression of pathogenic hSOD1 constructs does not alter ommatidia pigmentation or organization of all observed flies (at least 50 per genotype). C) Western blot analysis of Elav and Repo protein expression in non-mutant (elav-Gal4/+) and ALS (elav-Gal4 > UAS-hSOD1^{A4V} – elav-Gal4 > UAS-hSOD1^{G85R}) 0–3 days and17–20 days fly heads. Giotto protein was used as loading control. Results are expressed as means ± SEM of at least three independent biological replicates (as indicated by individual data points). Statistical significance was calculated by unpaired *t*-test (*p < 0.05; **p < 0.01). D) Confocal microscopy images showing immunofluorescence against Repo (panels *a*, *e*, *i*) and hSOD1 (panels *d* and *h*) on brains isolated from 0 to 3 days flies pan-neuronally expressing membrane-tethered GFP (to visualize neurons and neuropile – panels *b*, *f*, *j*) and ALS constructs (elav-Gal4 > UAS-mCD8:GFP; UAS-hSOD1^{A4V} – elav-Gal4 > UAS-mCD8:GFP; UAS-hSOD1^{G85R}) with age-matched control (elav-Gal4 > UAS-mCD8:GFP). DAPI was used to stain nuclei (panels *c*, *g*, *k*). Scale bar indicates 50 μM. Bar graph represents relative mean fluorescence ± SEM obtained by processing each image with ImageJ software. Individual data points correspond to each analyzed brain. Statistical significance was calculated by unpaired *t*-test (**p < 0.001).

hSOD1^{G85R} sample eliciting a stronger signal, but also exhibit the absence of evident neuronal loss (Fig. 2D, panels *b*, *f*, *j*), if compared with healthy brains (elav-Gal4 > UAS-mCD8:GFP). Moreover, the topographical distribution of Repo foci (at the interface between neuropil and neuronal bodies) seems typical of the fly astrocyte-like glia [52], thus corroborating the hypothesis of the presence of ALS-induced gliosis.

3.3. *hSOD1^{A4V} and hSOD1^{G85R} pan-neuronal expression activates an early immune response with AMPs up-regulation*

Drosophila antimicrobial peptides (AMPs) are evolutionarily conserved effector molecules in innate immunity, regulated by the Nf-κB-related pathways of Toll and immunodeficiency (IMD) [53–55]. Beyond their antimicrobial activity, AMPs have been recently reported to play important roles in the regulation of sleep, memory [56], ageing [57], neuroinflammation, and neurodegeneration [58,59].

Based on this knowledge, we decided to investigate AMPs transcripts expression as neuroinflammatory features of ALS pathogenesis in our *Drosophila* models. We evaluated AMPs expression by performing qRT-PCR on total RNA extracted from the heads of 0–3 and 17–20 days old flies. The analyzed AMPs were: attacin, cecropin, diptericin and drosocin (belonging to the IMD pathway) and defensin, drosomycin and metchnikowin (regulated by the Toll pathway). Our results demonstrate that flies with pan-neuronal expression of hSOD1^{A4V} show a significant and progressive increase of IMD-AMPs respect to non-mutant controls at both 0–3 and 17–20 days (Fig. 3A). On the other hand, flies with pan-neuronal expression of hSOD1^{G85R} show an increase of IMD-AMPs only at 0–3 days, but not at 17–20 days of age (Fig. 3B). Furthermore, Toll-AMPs show a significant up-regulation in hSOD1^{A4V} flies at early but not late time-points and, similarly it occurs with hSOD1^{G85R} flies that exhibit an increment of metchnikowin at 0–3 days.

These results link the pan-neuronal ectopic expression of hSOD1 mutants to a strong up-regulation of the innate immunity pathways and confirm the early inflammatory phenotype of these SOD1-ALS flies.

3.4. *Mutant hSOD1 enhances oxidative stress, impairs antioxidant defense and induces chromosome aberrations*

The excess of ROS or the reduced activity of the enzymes involved in the antioxidant defense are well recognized mechanisms of many CNS diseases, including ALS [60]. With the aim of further characterizing the early pathogenic features induced by pan-neuronal expression of mutant hSOD1, we measured the overall amount of generated ROS and the expression of the major antioxidant enzymes in ALS flies compared to non-mutant controls.

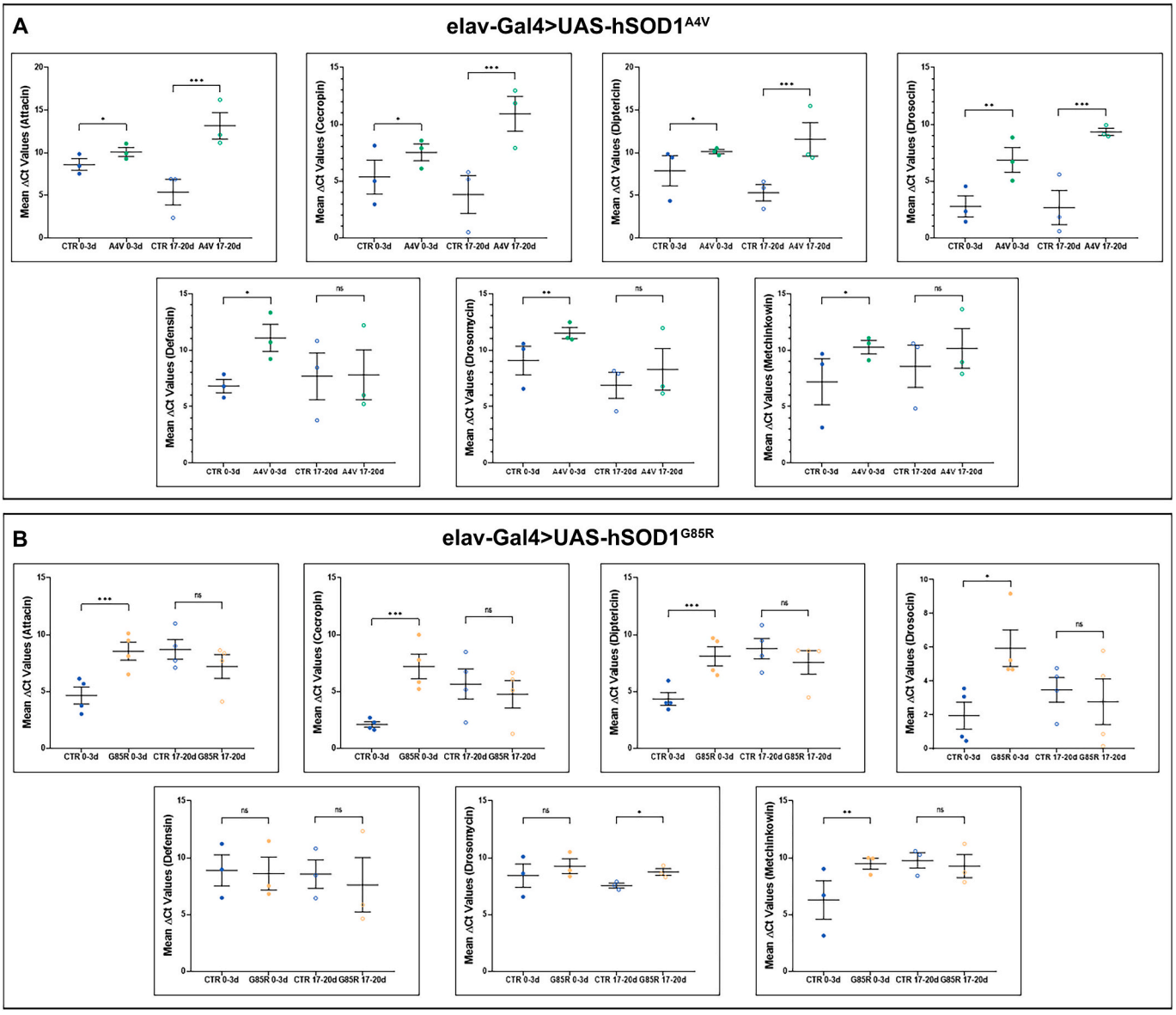

Fig. 3. hSOD1^{A4V} and hSOD1^{G85R} pan-neuronal expression up-regulates fly immune IMD pathway. qRT-PCR analysis of AMPs transcripts (attacin, cecropin, diptericin, drosocin, defensin, drosomycin and metchnikowin) in elav-Gal4 > UAS-hSOD1^{A4V} (Panel A, green circles) and elav-Gal4 > UAS-hSOD1^{G85R} (Panel B, orange circles) 0–3 days (full circles) and 17–20 days (empty circles) fly heads. Blue circles represent transcript levels of control flies, elav-Gal4/+ (CTR). Transcript levels were normalized to the housekeeping ribosomal *rp49*. Each circle in the charts represents the differential transcript expression (ΔCt) between the mRNA of interest and the *rp49* transcript and is an individual biological replicate (in turn obtained as the mean of three technical replicates). For all experiments, error bars indicate SEM. Statistical significance was calculated by unpaired two-tailed *t*-test (ns: not significant, *p < 0.05, **p < 0.01, ***p < 0.001).

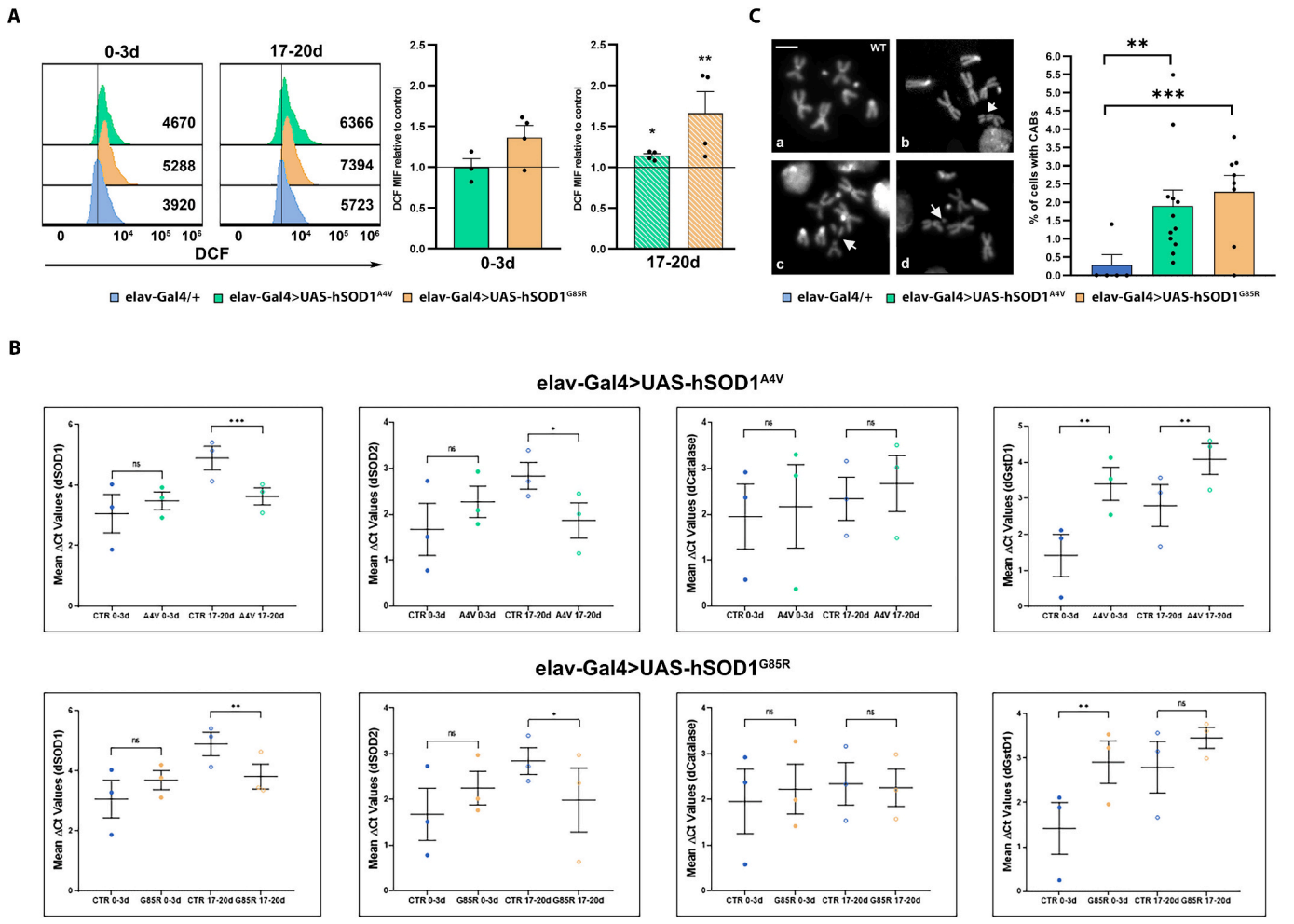

Fig. 4. hSOD1^{A4V} and hSOD1^{G85R} pan-neuronal expression alters fly oxidative balance and induces chromosome aberrations. A) Global ROS measurement from control (elav-Gal4/+) and ALS (elav-Gal4 > UAS-hSOD1^{A4V} – elav-Gal4 > UAS-hSOD1^{G85R}) 0–3 days and 17–20 days fly heads. The overlay histograms on the left are representative of the mean intensity fluorescence (MIF) of DCF. On the right, the cumulative data of intensity increase compared to the control (three experiments, as indicated by individual data points ± SEM). B) qRT-PCR analysis of fly antioxidant enzyme transcripts (Sod1, Sod2, Catalase and GstD1) in non-mutant (elav-Gal4/+, blue circles, CTR) and ALS (elav-Gal4 > UAS-hSOD1^{A4V}, green circles – elav-Gal4 > UAS-hSOD1^{G85R}, orange circles) 0–3 days (full circles) and 17–20 days (empty circles) fly heads. Transcript levels were normalized to *actin*. Each circle in the charts represents the differential transcript expression (ΔCt) between the mRNA of interest and the *actin* transcript and is an individual biological replicate (in turn obtained as the mean of three technical replicates). For all experiments, error bars indicate SEM. Statistical significance was calculated by unpaired two tailed *t*-test (ns: not significant, *p < 0.05, **p < 0.01, ***p < 0.001). C) Mitotic chromosomes from third instar larval non-mutant (elav-Gal4/+) and ALS brains (elav-Gal4 > UAS-hSOD1^{A4V} – elav-Gal4 > UAS-hSOD1^{G85R}) stained with DAPI. ALS metaphases show a higher frequency of chromosome aberrations if compared with control. Panels show a) wild-type (WT) karyotype, b) isochromatid deletion of a major autosome (arrow), c) centric deletion (arrow), d) chromatid deletion (arrow). Scale bar indicates 5 μM. Bar graph reports the scored frequency of chromosomal abnormalities observed in the analyzed metaphases. Individual data points represent each analyzed larval brain (for each brain were scored at least 500 cells). Statistical significance was obtained by Chi-square test with Bonferroni correction (**p < 0.01, ***p < 0.001).

We performed flow cytometric analysis to quantify 2′,7′-dichlorofluorescein (DCF), a fluorescent compound that is produced following the oxidation of 2′,7′-dichlorofluorescein diacetate (H_2DCF-DA) by ROS [61]. As reported in Fig. 4A, 0–3 and 17–20 days old hSOD1^{G85R} and 17–20 days old hSOD1^{A4V} flies show increased production of DCF compared to age-matched healthy controls, indicating a major degree of oxidative stress.

Moreover, we performed a qRT-PCR on total RNA obtained by fly heads to assess the expression of the key-components of *Drosophila* antioxidant and detoxifying enzymes: dSOD1 (*Drosophila* Sod1), dSOD2 (*Drosophila* Sod2), dCatalase (*Drosophila* Catalase) and dGstD1 (*Drosophila* Glutathione-S-Transferase D1). Fig. 4B indicates that dSod1 and dSod2 are significantly reduced only in 17–20 days old flies expressing either one of the pathogenic constructs. dGstD1, responsible for detoxifying both xenobiotic and endogenous compounds such as peroxidized lipids, is instead always significantly up-regulated in pan-neuronally expressing hSOD1^{A4V} flies, but only at 0–3 days in hSOD1^{G85R} flies. These results confirm that mutant hSOD1 enhances oxidative stress by augmenting ROS production and altering antioxidant enzymes transcription.

The *Drosophila* larval brain is the only neuronal tissue containing actively dividing neuroblasts, from which it is possible to isolate highly condensed metaphase chromosomes. In order to assess if pan-neuronal activation of mutant hSOD1 could induce glaring chromosome damage, we analyzed metaphase chromosomes in brains from third instar non-mutant and ALS larvae. We observed that ALS constructs induce high frequency of chromosome aberrations, such as isochromatid deletions (arrow in panel *b* – Fig. 4C), centric deletions (arrow in panel *c* – Fig. 4C) and chromatid deletions (arrowheads in panel *d* – Fig. 4C). In particular, mutant hSOD1 expression increases chromosome aberration frequency from 0.40 % (wild-type – panel *a* – Fig. 4C) to 1.89 % in hSOD1^{A4V} and to 2.28 % in hSOD1^{G85R} expressing larvae. Our results

demonstrate that pan-neuronal induction of hSOD1^{A4V} and hSOD1^{G85R} pathogenic constructs alters genomic integrity and causes chromosome aberrations.

4. Discussion

ALS is a rare and devastating disease, whose etiology is still largely to be deciphered, as well as the exact molecular progression of motor neuron degeneration and neuroinflammation as common features characterizing its pathogenesis [62–67].

In our current study, we have chosen to express hSOD1^{A4V} or hSOD1^{G85R} ALS transgenes selectively in all neurons of *Drosophila*, with the aim to dissect their specific contribution to the pathogenesis. We are conscious that ALS is a non-cell autonomous disease and patients carry the mutation in all cells. On the other hand, we firmly believe that by dissecting one at the time the contribution of each single cell phenotype, we can progressively gain important insight on ALS global mechanisms. In order to legitimate our new models, among the overt pathological traits we started investigating the lifespan, which in patients is severely affected since the majority of them lives on average between 2 and 5 years from diagnosis [68]. We have established that the pathogenic constructs hSOD1^{A4V} and hSOD1^{G85R} when expressed pan-neuronally share strong detrimental effects on fly survival, albeit at different levels, with A4V flies being more susceptible to death than G85R flies. This result compared to previous work represents a first improvement in reproducing ALS susceptibility to death, because ectopic expression of these same constructs exclusively in motor neurons [22,69], or in glia [70], does not cause significative decrease of median survival.

In order to characterize our hSOD1 pan-neuronally expressing models, we next evaluated the climbing activity of *Drosophila* in response to the negative geotaxic reflex. To date, it is well-documented that motor neuron expression of hSOD1^{G85R} alters fly locomotor abilities, determining about 50 % reduction of the climbing success at 28 days post-eclosion [69,71–74], but there is no evidence concerning the pan-neuronal induction of hSOD1^{G85R} as well as hSOD1^{A4V} constructs. We established that the expression of hSOD1^{A4V} and hSOD1^{G85R} in all neurons induces motor impairment both at 0–3 days (about 20 % reduction) and 17–20 days (about 50 % reduction) of age, thus representing a further validation of our new models in reproducing ALS features.

Because motor neuron degeneration is known to be incremental and cumulative over time and minor motor disabilities are initially insufficient to allow definite diagnostic recognition, ALS is often characterized by an invariably long delay between the silent onset of symptoms and the diagnosis. This prodromal time is regrettably always missed. In an attempt to fill this information gap, we mostly concentrated our study on early time points to identify those signs that are generally unexploited. We observed that motor impairment can for instance occur in the apparent absence of neurodegeneration, as established by the perfectly preserved ommatidial morphology and pigmentation obtained after the expression of the pathogenic constructs not only in all neurons, but also directly in the eye. The absence of neurodegeneration is further confirmed by the constant expression of the neuronal marker Elav in hSOD1^{A4V} and hSOD1^{G85R} fly heads. It is important to remark that these ALS flies do not show neurodegeneration in the brain until the late time that we tested (25–28 days – data not shown). Of note, also in the SOD1^{G85R} mouse model the primary motor neurons in the brain only show mild signs of suffering, while conspicuous neuronal loss begins to be observed only after eight months [14]. However, we do not exclude that neurodegeneration might be present in the thoracic ganglion (roughly corresponding to the spinal cord in vertebrates) or that another site of dysfunction might be represented by the synapses.

In determining the progressive and cumulative transition toward the phenotypically manifest climbing impairment, we evaluated neuroinflammation and detected the up-regulation of the glia marker Repo and the activation of the NF-κB-related AMPs immune pathway. While NF-κB is a master regulator of immune responses and neuroinflammation also in *Drosophila* [75], only recent work instead describes an association between fly AMPs up-regulation and neuroinflammation. In addition to the defense against pathogens, AMPs guarantee the correct functioning of the nervous system playing a prominent role in the cross-talk between innate immunity and neural activity [55]. AMPs are also found in vertebrates and particularly in human [76,77]. Interestingly, our work is the first to establish a correlation between SOD1 mutations and AMPs that are instead known to be up-regulated in *Drosophila* models of neurodegeneration/neuroinflammation such as ataxia telangiectasia [78], Alzheimer's Disease [79], and traumatic brain injury [80]. Thus, our results now introduce attacin, cecropin, diptericin, drosocin, defensin, drosomycin and metchnikowin as novel biological mediators/markers of the neuroimmune-glia signaling and of the early evolution of the SOD1-ALS phenotype [81]. Confirming our results, pan-neuronal or motor neuronal overexpression of human TAR DNA-binding Protein 43 (TDP-43), a major pathological protein in ALS, leads to up-regulation of attacin and diptericin, and to a minor extent also of cecropin and drosocin [82]. Remarkably, downregulation of the antimicrobial Toll-related peptide metchinkowin suppresses poly-(GR)-induced neurotoxicity in C9ORF72-ALS fly model [83]. On this regard, the aim of our future work will be to screen if downregulation of attacin, cecropin, diptericin, drosocin, defensin, drosomycin or metchnikowin in our hSOD1 models can similarly induce beneficial effects.

It is well known that redox biochemistry represents an important mechanism of SOD1-ALS and that neurons are particularly sensitive to oxidative stress [16]. Moreover, an altered oxidative balance in terms of scarce antioxidant defense and abundant unbuffered ROS is found in the SOD1-G93A murine model, human and yeast SOD1 models [84], and also in SOD1 patients [85–87]. Our results, establishing increased oxidative stress and dysregulation of antioxidant enzymes after pan-neuronal expression of hSOD1^{A4V} and hSOD1^{G85R} transgenes, corroborate previous work and further characterize our flies as a proficient model where to investigate SOD1-ALS pathogenesis. Moreover, our results identify particularly GstD1 as a promising early transcript to be further investigated for dissecting the SOD1-ALS evolution. Not surprisingly, Gst omega 2 is involved in neurotoxicity in a hTDP-43 *Drosophila* model [88].

Correlations between oxidative stress and DNA damage in ALS are recognized as important pathogenic mechanisms [89,90]. High levels of 8-oxo-2′-deoxyguanosine, a marker of oxidated DNA, were reported in fALS and sALS patients [91], and in SOD1^{G93A} murine [92] and cellular models [93]. Moreover, an increased histone γH2AX variant, marker of double strand breaks, was detected in SOD1^{G93A} and SOD1^{A4V} patient-derived iPSC lines [89]. Corroborating these results, our work constitutes the first evidence of a direct correlation between SOD1^{G85R}/SOD1^{A4V} mutations and structural chromosome damage in *Drosophila* larvae. If validated in higher organisms and especially in patients, the presence of chromosome aberrations might contribute to untangle the clinically silent phase eventually evolving into clinically manifest ALS symptoms and, most importantly, to reduce the disastrous delay among early symptoms, definite diagnosis, and likely beginning of therapy that is now the norm for most ALS patients.

5. Conclusions

Our work has established that despite shared effects on reduced survival and impaired motor performance, the pan-neuronal expression of *SOD1* transgenes in *Drosophila* induces neuroinflammatory phenotypes that are slightly different in terms of timing (0–3 versus 17–20 days) and intensity in SOD1^{G85R} versus SOD1^{A4V} flies. Repo is transiently increased at 0–3 days, while Sod1/Sod2 are instead similarly decreased at 17–20 days in both fly models; GstD1 and AMPs are up-regulated early but transiently in G85R, while permanently in A4V; finally, ROS are augmented permanently in G85R and only late in A4V (Table 1). This could mean that the precarious balance between

Table 1
Synoptic view of investigated parameters modulated by pan-neuronal expression of ALS hSOD1^{A4V} or hSOD1^{G85R} constructs in *Drosophila*.

Genotype	elav-Gal4>UAS-hSOD1^{A4V}		elav-Gal4>UAS-hSOD1^{G85R}		Figs.
Time-point	0–3 days	17–20 days	0–3 days	17–20 days	
Motor performance	↓	↓	↓	↓	1B
Elav	=	=	=	=	2C
Repo	↑	=	↑	=	2C/2D
Attacin	↑	↑	↑	=	3A/3B
Cecropin	↑	↑	↑	=	3A/3B
Diptericin	↑	↑	↑	=	3A/3B
Drosocin	↑	↑	↑	=	3A/3B
Defensin	↑	=	=	=	3A/3B
Drosomycin	↑	=	=	=	3A/3B
Metchnikowin	↑	=	↑	=	3A/3B
ROS	=	↑	↑	↑	4A
Sod1/Sod2	=	↓	=	↓	4B
Catalase	=	=	=	=	4B
GstD1	↑	↑	↑	=	4B
Chromosome aberrations (larval brain)	↑		↑		4C

In this table we describe the biological parameters that are modulated in all neurons after ALS mutant transgene expression. Up-regulation is represented by ↑ arrow, down-regulation by ↓ arrow, unchanged values by =.

pathological initiators and propagators might be somehow different in the two transgene lines, being diverse the impact that different mutations distributed throughout the gene might have on a variety of protein domains and functions.

In trying to describe the still indeterminate but incremental transition between an unaffected state and an acclaimed ALS, our work has moreover provided a unique opportunity to shed light on some of the earliest molecular features of *SOD1^{G85R}/SOD1^{A4V}* mutations, at least in *Drosophila*. On the basis of our results, it is now clear that particularly chromosome aberrations, in addition to modulation of AMPs and GstD1 might constitute previously unexplored mechanisms and open an exciting new venue of research on the detection of biomarkers for the patient silent phase of the disease.

Supplementary data to this article can be found online at https://doi.org/10.1016/j.bbadis.2024.167192.

Ethical approval and consent to participate

Not applicable.

Funding

This study was supported by FaTALSDRUG project SAC. AD002.173.058 from National Research Council Progetti di Ricerca@CNR to C.V.

CRediT authorship contribution statement

Francesco Liguori: Writing – review & editing, Writing – original draft, Investigation, Formal analysis, Conceptualization. **Francesca Alberti:** Investigation. **Susanna Amadio:** Investigation, Formal analysis. **Daniela Francesca Angelini:** Investigation. **Eleonora Pilesi:** Investigation. **Giuseppe Vitale:** Investigation. **Giulia Tesoriere:** Investigation. **Giovanna Borsellino:** Writing – review & editing. **Fiammetta Vernì:** Writing – review & editing, Formal analysis. **Cinzia Volonté:** Writing – review & editing, Writing – original draft, Funding acquisition, Formal analysis, Conceptualization.

Declaration of competing interest

The authors declare no competing interests.

Data availability

All data generated or analyzed during this study are included in this published article and its supplementary information files.

Acknowledgements

We are indebted with Prof. Udai Pandey for the gift of transgenic FUS flies and with Prof. Lucia Piacentini for BL5146 fly stock. We are grateful to Dr. A. Mattioni and Dr. F. Strappazzon (Fondazione Santa Lucia, Rome) for anti-Giotto antibody. We appreciated the kind assistance of Dr. S. Scaricamazza (Fondazione Santa Lucia, Rome) for statistical calculations and representations.

This work is dedicated to the late esteemed colleague Professor Justin J. Yerbury, in recognition of his huge courage, optimism, and outstanding contribution and commitment to defeat motor neuron disease. All lives are meaningful and some are extraordinary, not only in achievements and capabilities, as in the wondrous power with which they are carried on. This was Justin's life.

Consent for publication

Not applicable.

References

[1] A. Chiò, G. Mora, A. Calvo, L. Mazzini, E. Bottacchi, R. Mutani, PARALS, epidemiology of ALS in Italy: a 10-year prospective population-based study, Neurology 72 (8) (2009) 725–731.
[2] F. Akçimen, E.R. Lopez, J.E. Landers, A. Nath, A. Chiò, R. Chia, B.J. Traynor, Amyotrophic lateral sclerosis: translating genetic discoveries into therapies, Nat. Rev. Genet. 24 (2023) 642–658.
[3] H.P. Nguyen, C. Van Broeckhoven, J. van der Zee, ALS genes in the genomic era and their implications for FTD, Trends Genet. 34 (6) (2018) 404–423.
[4] A.A. Alsultan, R. Waller, P.R. Heath, J. Kirby, The genetics of amyotrophic lateral sclerosis: current insights, Degener Neurol Neuromuscul Dis 6 (2016) 49–64.
[5] A. Shatunov, A. Al-Chalabi, The genetic architecture of ALS, Neurobiol. Dis. 147 (2021) 105156.
[6] D.R. Rosen, T. Siddique, D. Patterson, D.A. Figlewicz, P. Sapp, A. Hentati, D. Donaldson, J. Goto, J.P. O'Regan, H.X. Deng, Mutations in Cu/Zn superoxide dismutase gene are associated with familial amyotrophic lateral sclerosis, Nature 362 (6415) (1993) 59–62.
[7] O. Abel, J.F. Powell, P.M. Andersen, A. Al-Chalabi, ALSoD: a user-friendly online bioinformatics tool for amyotrophic lateral sclerosis genetics, Hum. Mutat. 33 (9) (2012) 1345–1351.
[8] G. Marangi, B.J. Traynor, Genetic causes of amyotrophic lateral sclerosis: new genetic analysis methodologies entailing new opportunities and challenges, Brain Res. 1607 (2015) 75–93.

[9] M.J. Parton, W. Broom, P.M. Andersen, A. Al-Chalabi, P. Nigel Leigh, J.F. Powell, C.E. Shaw, D.A.S.A. Consortium, D90A-SOD1 mediated amyotrophic lateral sclerosis: a single founder for all cases with evidence for a Cis-acting disease modifier in the recessive haplotype, Hum. Mutat. 20 (6) (2002) 473.

[10] P. Mondola, M. Santillo, R. Serù, S. Damiano, C. Alvino, G. Ruggiero, P. Formisano, G. Terrazzano, A. Secondo, L. Annunziato, Cu,Zn superoxide dismutase increases intracellular calcium levels via a phospholipase C-protein kinase C pathway in SK-N-BE neuroblastoma cells, Biochem. Biophys. Res. Commun. 324 (2) (2004) 887–892.

[11] D.G. Franchina, C. Dostert, D. Brenner, Reactive oxygen species: involvement in T cell signaling and metabolism, Trends Immunol. 39 (6) (2018) 489–502.

[12] S. Damiano, A. Sasso, R. Accetta, M. Monda, B. De Luca, L.M. Pavone, A. Belfiore, M. Santillo, P. Mondola, Effect of mutated Cu, Zn superoxide dismutase (SOD1 G93A) on modulation of Transductional pathway mediated by M1 muscarinic receptor in SK-N-BE and NSC-34 cells, Front. Physiol. 9 (2018) 611.

[13] P. Mondola, S. Damiano, A. Sasso, M. Santillo, The Cu, Zn superoxide dismutase: not only a dismutase enzyme, Front. Physiol. 7 (2016) 594.

[14] L.I. Bruijn, M.W. Becher, M.K. Lee, K.L. Anderson, N.A. Jenkins, N.G. Copeland, S. S. Sisodia, J.D. Rothstein, D.R. Borchelt, D.L. Price, D.W. Cleveland, ALS-linked SOD1 mutant G85R mediates damage to astrocytes and promotes rapidly progressive disease with SOD1-containing inclusions, Neuron 18 (2) (1997) 327–338.

[15] R.J. Mockett, S.N. Radyuk, J.J. Benes, W.C. Orr, R.S. Sohal, Phenotypic effects of familial amyotrophic lateral sclerosis mutant Sod alleles in transgenic Drosophila, Proc. Natl. Acad. Sci. U. S. A. 100 (1) (2003) 301–306.

[16] S. Boillée, C. Vande Velde, D.W. Cleveland, ALS: a disease of motor neurons and their nonneuronal neighbors, Neuron 52 (1) (2006) 39–59.

[17] H. Ilieva, M. Polymenidou, D.W. Cleveland, Non-cell autonomous toxicity in neurodegenerative disorders: ALS and beyond, J. Cell Biol. 187 (6) (2009) 761–772.

[18] S.J. Kaur, S.R. McKeown, S. Rashid, Mutant SOD1 mediated pathogenesis of amyotrophic lateral sclerosis, Gene 577 (2) (2016) 109–118.

[19] C. Volonté, S. Apolloni, M. Sabatelli, Histamine beyond its effects on allergy: potential therapeutic benefits for the treatment of Amyotrophic Lateral Sclerosis (ALS), Pharmacol. Ther. 202 (2019) 120–131.

[20] V. Rubino, G. La Rosa, L. Pipicelli, F. Carriero, S. Damiano, M. Santillo, G. Terrazzano, G. Ruggiero, P. Mondola, Insights on the multifaceted roles of wild-type and mutated superoxide dismutase 1 in amyotrophic lateral sclerosis pathogenesis, Antioxidants (Basel) 12 (9) (2023).

[21] F. Liguori, S. Amadio, C. Volonté, Where and why modeling amyotrophic lateral sclerosis, Int. J. Mol. Sci. 22 (8) (2021).

[22] M.R. Watson, R.D. Lagow, K. Xu, B. Zhang, N.M. Bonini, A drosophila model for amyotrophic lateral sclerosis reveals motor neuron damage by human SOD1, J. Biol. Chem. 283 (36) (2008) 24972–24981.

[23] H.X. Deng, A. Hentati, J.A. Tainer, Z. Iqbal, A. Cayabyab, W.Y. Hung, E.D. Getzoff, P. Hu, B. Herzfeldt, R.P. Roos, Amyotrophic lateral sclerosis and structural defects in Cu,Zn superoxide dismutase, Science 261 (5124) (1993) 1047–1051.

[24] M. Saeed, Y. Yang, H.X. Deng, W.Y. Hung, N. Siddique, L. Dellefave, C. Gellera, P. M. Andersen, T. Siddique, Age and founder effect of SOD1 A4V mutation causing ALS, Neurology 72 (19) (2009) 1634–1639.

[25] T. Juneja, M.A. Pericak-Vance, N.G. Laing, S. Dave, T. Siddique, Prognosis in familial amyotrophic lateral sclerosis: progression and survival in patients with glu100gly and ala4val mutations in Cu,Zn superoxide dismutase, Neurology 48 (1) (1997) 55–57.

[26] M.E. Cudkowicz, D. McKenna-Yasek, P.E. Sapp, W. Chin, B. Geller, D.L. Hayden, D. A. Schoenfeld, B.A. Hosler, H.R. Horvitz, R.H. Brown, Epidemiology of mutations in superoxide dismutase in amyotrophic lateral sclerosis, Ann. Neurol. 41 (2) (1997) 210–221.

[27] D.R. Rosen, A.C. Bowling, D. Patterson, T.B. Usdin, P. Sapp, E. Mezey, D. McKenna-Yasek, J. O'Regan, Z. Rahmani, R.J. Ferrante, A frequent ala 4 to val superoxide dismutase-1 mutation is associated with a rapidly progressive familial amyotrophic lateral sclerosis, Hum. Mol. Genet. 3 (6) (1994) 981–987.

[28] L.J. Hayward, J.A. Rodriguez, J.W. Kim, A. Tiwari, J.J. Goto, D.E. Cabelli, J. S. Valentine, R.H. Brown, Decreased metallation and activity in subsets of mutant superoxide dismutases associated with familial amyotrophic lateral sclerosis, J. Biol. Chem. 277 (18) (2002) 15923–15931.

[29] F. Liguori, S. Amadio, C. Volonté, Fly for ALS: Drosophila modeling on the route to amyotrophic lateral sclerosis modifiers, Cell. Mol. Life Sci. 78 (17–18) (2021) 6143–6160.

[30] I. Casci, U.B. Pandey, A fruitful endeavor: modeling ALS in the fruit fly, Brain Res. 1607 (2015) 47–74.

[31] K.N. Hegde, A. Srivastava, Drosophila melanogaster as a tool for amyotrophic lateral sclerosis research, J Dev Biol 10 (3) (2022).

[32] G. Prelich, Gene overexpression: uses, mechanisms, and interpretation, Genetics 190 (3) (2012) 841–854.

[33] N.A. Lanson, A. Maltare, H. King, R. Smith, J.H. Kim, J.P. Taylor, T.E. Lloyd, U. B. Pandey, A Drosophila model of FUS-related neurodegeneration reveals genetic interaction between FUS and TDP-43, Hum. Mol. Genet. 20 (13) (2011) 2510–2523.

[34] N.J. Linford, C. Bilgir, J. Ro, S.D. Pletcher, Measurement of lifespan in Drosophila melanogaster, J. Vis. Exp. 71 (2013).

[35] S.K. Han, D. Lee, H. Lee, D. Kim, H.G. Son, J.S. Yang, S.V. Lee, S. Kim, OASIS 2: online application for survival analysis 2 with features for the analysis of maximal lifespan and healthspan in aging research, Oncotarget 7 (35) (2016) 56147–56152.

[36] S.B. Manjila, G. Hasan, Flight and climbing assay for assessing motor functions in Drosophila, Bio-Protoc. 8 (5) (2018) e2742.

[37] M.G. Giansanti, S. Bonaccorsi, R. Kurek, R.M. Farkas, P. Dimitri, M.T. Fuller, M. Gatti, The class I PITP giotto is required for Drosophila cytokinesis, Curr. Biol. 16 (2) (2006) 195–201.

[38] M.K. Gatt, D.M. Glover, The Drosophila phosphatidylinositol transfer protein encoded by vibrator is essential to maintain cleavage-furrow ingression in cytokinesis, J. Cell Sci. 119 (Pt 11) (2006) 2225–2235.

[39] A.M. Casale, F. Liguori, F. Ansaloni, U. Cappucci, S. Finaurini, G. Spirito, F. Persichetti, R. Sanges, S. Gustincich, L. Piacentini, Transposable element activation promotes neurodegeneration in a Drosophila model of Huntington's disease, iScience 25 (1) (2022) 103702.

[40] G. Bosso, F. Cipressa, M.L. Moroni, R. Pennisi, J. Albanesi, V. Brandi, S. Cugusi, F. Renda, L. Ciapponi, F. Polticelli, A. Antoccia, A. di Masi, G. Cenci, NBS1 interacts with HP1 to ensure genome integrity, Cell Death Dis. 10 (12) (2019) 951.

[41] E. Mascolo, F. Liguori, L. Stufera Mecarelli, N. Amoroso, C. Merigliano, S. Amadio, C. Volonté, R. Contestabile, A. Tramonti, F. Vernì, Functional inactivation of Drosophila GCK orthologs causes genomic instability and oxidative stress in a fly model of MODY-2, Int. J. Mol. Sci. 22 (2) (2021).

[42] R. Rout, S. Basu, M. Mishra, Reactive oxygen species detection of Drosophila cells by flow cytometry, in: M. Mishra (Ed.), Fundamental Approaches to Screen Abnormalities in Drosophila, Springer, 2020, pp. 97–109.

[43] E. Pilesi, C. Angioli, C. Graziani, A. Parroni, R. Contestabile, A. Tramonti, F. Vernì, A gene-nutrient interaction between vitamin B6 and serine hydroxymethyltransferase (SHMT) affects genome integrity in Drosophila, J. Cell. Physiol. 238 (2023) 1558–1566.

[44] A.H. Brand, N. Perrimon, Targeted gene expression as a means of altering cell fates and generating dominant phenotypes, Development 118 (2) (1993) 401–415.

[45] S. Robinow, K. White, The locus elav of Drosophila melanogaster is expressed in neurons at all developmental stages, Dev. Biol. 126 (2) (1988) 294–303.

[46] M. Mishra, E. Knust, Analysis of the Drosophila compound eye with light and electron microscopy, Methods Mol. Biol. 935 (2013) 161–182.

[47] S. Mizielinska, S. Grönke, T. Niccoli, C.E. Ridler, E.L. Clayton, A. Devoy, T. Moens, F.E. Norona, I.O.C. Woollacott, J. Pietrzyk, K. Cleverley, A.J. Nicoll, S. Pickering-Brown, J. Dols, M. Cabecinha, O. Hendrich, P. Fratta, E.M.C. Fisher, L. Partridge, A. M. Isaacs, C9orf72 repeat expansions cause neurodegeneration in Drosophila through arginine-rich proteins, Science 345 (6201) (2014) 1192–1194.

[48] B.D. Freibaum, Y. Lu, R. Lopez-Gonzalez, N.C. Kim, S. Almeida, K.H. Lee, N. Badders, M. Valentine, B.L. Miller, P.C. Wong, L. Petrucelli, H.J. Kim, F.B. Gao, J.P. Taylor, GGGGCC repeat expansion in C9orf72 compromises nucleocytoplasmic transport, Nature 525 (7567) (2015) 129–133.

[49] M.C. Ellis, E.M. O'Neill, G.M. Rubin, Expression of Drosophila glass protein and evidence for negative regulation of its activity in non-neuronal cells by another DNA-binding protein, Development 119 (3) (1993) 855–865.

[50] R.M. Ransohoff, How neuroinflammation contributes to neurodegeneration, Science 353 (6301) (2016) 777–783.

[51] S. Apolloni, P. Fabbrizio, S. Amadio, C. Volonté, Actions of the antihistaminergic clemastine on presymptomatic SOD1-G93A mice ameliorate ALS disease progression, J. Neuroinflammation 13 (1) (2016) 191.

[52] M.C. Kremer, C. Jung, S. Batelli, G.M. Rubin, U. Gaul, The glia of the adult Drosophila nervous system, Glia 65 (4) (2017) 606–638.

[53] J.L. Imler, P. Bulet, Antimicrobial peptides in Drosophila: structures, activities and gene regulation, Chem. Immunol. Allergy 86 (2005) 1–21.

[54] S.H. Lye, S. Chtarbanova, Drosophila as a model to study brain innate immunity in health and disease, Int. J. Mol. Sci. 19 (12) (2018).

[55] S. Stączek, M. Cytryńska, A. Zdybicka-Barabas, Unraveling the role of antimicrobial peptides in insects, Int. J. Mol. Sci. 24 (6) (2023).

[56] S. Dissel, L. Seugnet, M.S. Thimgan, N. Silverman, V. Angadi, P.V. Thacher, M. M. Burnham, P.J. Shaw, Differential activation of immune factors in neurons and glia contribute to individual differences in resilience/vulnerability to sleep disruption, Brain Behav. Immun. 47 (2015) 75–85.

[57] B. Shit, A. Prakash, S. Sarkar, P.F. Vale, I. Khan, Ageing leads to reduced specificity of antimicrobial peptide responses in *Drosophila melanogaster*, Proc. Biol. Sci. 289 (1987) (2022) 20221642.

[58] S.K. Dubey, M.G. Tapadia, Yorkie regulates neurodegeneration through canonical pathway and innate immune response, Mol. Neurobiol. 55 (2) (2018) 1193–1207.

[59] N. Nayak, M. Mishra, Drosophila melanogaster as a model to understand the mechanisms of infection mediated neuroinflammation in neurodegenerative diseases, J. Integr. Neurosci. 21 (2) (2022) 66.

[60] E. Niedzielska, I. Smaga, M. Gawlik, A. Moniczewski, P. Stankowicz, J. Pera, M. Filip, Oxidative stress in neurodegenerative diseases, Mol. Neurobiol. 53 (6) (2016) 4094–4125.

[61] H. Possel, H. Noack, W. Augustin, G. Keilhoff, G. Wolf, 2,7-Dihydrodichlorofluorescein diacetate as a fluorescent marker for peroxynitrite formation, FEBS Lett. 416 (2) (1997) 175–178.

[62] I.A. Lambert-Smith, D.N. Saunders, J.J. Yerbury, Proteostasis impairment and ALS, Prog. Biophys. Mol. Biol. 174 (2022) 3–27.

[63] L. McAlary, Y.L. Chew, J.S. Lum, N.J. Geraghty, J.J. Yerbury, N.R. Cashman, Amyotrophic lateral sclerosis: proteins, proteostasis, prions, and promises, Front Cell Neurosci 14 (2020) 581907.

[64] J.J. Yerbury, N.E. Farrawell, L. McAlary, Proteome homeostasis dysfunction: a unifying principle in ALS pathogenesis, Trends Neurosci. 43 (5) (2020) 274–284.

[65] F. De Marchi, T. Franjkic, P. Schito, T. Russo, J. Nimac, A.A. Chami, A. Mele, L. Vidatic, J. Kriz, J.P. Julien, G. Apic, R.B. Russell, B. Rogelj, J.R. Cannon, M. Baralle, F. Agosta, S. Hecimovic, L. Mazzini, E. Buratti, I. Munitic, Emerging trends in the field of inflammation and proteinopathy in ALS/FTD spectrum disorder, Biomedicines 11 (6) (2023).

[66] C. Parisi, G. Napoli, S. Amadio, A. Spalloni, S. Apolloni, P. Longone, C. Volonté, MicroRNA-125b regulates microglia activation and motor neuron death in ALS, Cell Death Differ. 23 (3) (2016) 531–541.
[67] C. Volonté, S. Amadio, Amyotrophic lateral sclerosis disease burden: doing better at getting better, Neural Regen. Res. 18 (8) (2023) 1728–1729.
[68] L. Tzeplaeff, S. Wilfling, M.V. Requardt, M. Herdick, Current state and future directions in the therapy of ALS, Cells 12 (11) (2023).
[69] C. Zhang, W. Liang, H. Wang, Y. Yang, T. Wang, S. Wang, X. Wang, Y. Wang, H. Feng, γ-Oryzanol mitigates oxidative stress and prevents mutant SOD1-related neurotoxicity in Drosophila and cell models of amyotrophic lateral sclerosis, Neuropharmacology 160 (2019) 107777.
[70] R. Islam, E.L. Kumimoto, H. Bao, B. Zhang, ALS-linked SOD1 in glial cells enhances ß-N-methylamino L-alanine (BMAA)-induced toxicity in Drosophila, F1000Res 1 (2012) 47.
[71] F. De Rose, R. Marotta, G. Talani, T. Catelani, P. Solari, S. Poddighe, G. Borghero, F. Marrosu, E. Sanna, S. Kasture, E. Acquas, A. Liscia, Differential effects of phytotherapic preparations in the hSOD1 Drosophila melanogaster model of ALS, Sci. Rep. 7 (2017) 41059.
[72] T. Wang, J. Cheng, S. Wang, X. Wang, H. Jiang, Y. Yang, Y. Wang, C. Zhang, W. Liang, H. Feng, α-Lipoic acid attenuates oxidative stress and neurotoxicity via the ERK/Akt-dependent pathway in the mutant hSOD1 related Drosophila model and the NSC34 cell line of amyotrophic lateral sclerosis, Brain Res. Bull. 140 (2018) 299–310.
[73] T.H. Wang, S.Y. Wang, X.D. Wang, H.Q. Jiang, Y.Q. Yang, Y. Wang, J.L. Cheng, C. T. Zhang, W.W. Liang, H.L. Feng, Fisetin exerts antioxidant and neuroprotective effects in multiple mutant hSOD1 models of amyotrophic lateral sclerosis by activating ERK, Neuroscience 379 (2018) 152–166.
[74] C. Zhang, Y. Yang, W. Liang, T. Wang, S. Wang, X. Wang, Y. Wang, H. Jiang, H. Feng, Neuroprotection by urate on the mutant hSOD1-related cellular and Drosophila models of amyotrophic lateral sclerosis: implication for GSH synthesis via activating Akt/GSK3β/Nrf2/GCLC pathways, Brain Res. Bull. 146 (2019) 287–301.
[75] S. Minakhina, R. Steward, Nuclear factor-kappa B pathways in Drosophila, Oncogene 25 (51) (2006) 6749–6757.
[76] X. Kang, F. Dong, C. Shi, S. Liu, J. Sun, J. Chen, H. Li, H. Xu, X. Lao, H. Zheng, DRAMP 2.0, an updated data repository of antimicrobial peptides, Sci Data 6 (1) (2019) 148.
[77] Q.Y. Zhang, Z.B. Yan, Y.M. Meng, X.Y. Hong, G. Shao, J.J. Ma, X.R. Cheng, J. Liu, J. Kang, C.Y. Fu, Antimicrobial peptides: mechanism of action, activity and clinical potential, Mil. Med. Res. 8 (1) (2021) 48.
[78] A.J. Petersen, R.J. Katzenberger, D.A. Wassarman, The innate immune response transcription factor relish is necessary for neurodegeneration in a Drosophila model of ataxia-telangiectasia, Genetics 194 (1) (2013) 133–142.
[79] A. Barati, R. Masoudi, R. Yousefi, M. Monsefi, A. Mirshafiey, Tau and amyloid beta differentially affect the innate immune genes expression in Drosophila models of Alzheimer's disease and β-D Mannuronic acid (M2000) modulates the dysregulation, Gene 808 (2022) 145972.
[80] R.J. Katzenberger, C.A. Loewen, D.R. Wassarman, A.J. Petersen, B. Ganetzky, D. A. Wassarman, A Drosophila model of closed head traumatic brain injury, Proc. Natl. Acad. Sci. U. S. A. 110 (44) (2013) E4152–E4159.
[81] C.A. Mangold, D.P. Hughes, Insect behavioral change and the potential contributions of neuroinflammation-a call for future research, Genes (Basel) 12 (4) (2021).
[82] L. Zhan, Q. Xie, R.S. Tibbetts, Opposing roles of p38 and JNK in a Drosophila model of TDP-43 proteinopathy reveal oxidative stress and innate immunity as pathogenic components of neurodegeneration, Hum. Mol. Genet. 24 (3) (2015) 757–772.
[83] S. Lee, Y.W. Jun, G.R. Linares, B. Butler, Y. Yuva-Adyemir, J. Moore, G. Krishnan, B. Ruiz-Juarez, M. Santana, M. Pons, N. Silverman, Z. Weng, J.K. Ichida, F.B. Gao, Downregulation of Hsp90 and the antimicrobial peptide Mtk suppresses poly(GR)-induced neurotoxicity in C9ORF72-ALS/FTD, Neuron 111 (9) (2023) 1381–1390. e6.
[84] A.A. Brasil, M.D.C. de Carvalho, E. Gerhardt, D.D. Queiroz, M.D. Pereira, T. F. Outeiro, E.C.A. Eleutherio, Characterization of the activity, aggregation, and toxicity of heterodimers of WT and ALS-associated mutant Sod1, Proc. Natl. Acad. Sci. U. S. A. 116 (51) (2019) 25991–26000.
[85] Y. Furukawa, R. Fu, H.X. Deng, T. Siddique, T.V. O'Halloran, Disulfide cross-linked protein represents a significant fraction of ALS-associated cu, Zn-superoxide dismutase aggregates in spinal cords of model mice, Proc. Natl. Acad. Sci. U. S. A. 103 (18) (2006) 7148–7153.
[86] A. Nikolić-Kokić, Z. Stević, D. Blagojević, B. Davidović, D.R. Jones, M.B. Spasić, Alterations in anti-oxidative defence enzymes in erythrocytes from sporadic amyotrophic lateral sclerosis (SALS) and familial ALS patients, Clin. Chem. Lab. Med. 44 (5) (2006) 589–593.
[87] S. Apolloni, P. Fabbrizio, C. Parisi, S. Amadio, C. Volonté, Clemastine confers neuroprotection and induces an anti-inflammatory phenotype in SOD1(G93A) mouse model of amyotrophic lateral sclerosis, Mol. Neurobiol. 53 (1) (2016) 518–531.
[88] S.J. Cha, Y.J. Han, H.J. Choi, H.J. Kim, K. Kim, Glutathione S-transferase rescues motor neuronal toxicity in fly model of amyotrophic lateral sclerosis, Antioxidants (Basel) 9 (7) (2020).
[89] B.W. Kim, Y.E. Jeong, M. Wong, L.J. Martin, DNA damage accumulates and responses are engaged in human ALS brain and spinal motor neurons and DNA repair is activatable in iPSC-derived motor neurons with SOD1 mutations, Acta Neuropathol. Commun. 8 (1) (2020) 7.
[90] A. Konopka, J.D. Atkin, D.N.A. Damage, Defective DNA repair, and neurodegeneration in amyotrophic lateral sclerosis, Front. Aging Neurosci. 14 (2022) 786420.
[91] M. Bogdanov, R.H. Brown, W. Matson, R. Smart, D. Hayden, H. O'Donnell, M. Flint Beal, M. Cudkowicz, Increased oxidative damage to DNA in ALS patients, Free Radic. Biol. Med. 29 (7) (2000) 652–658.
[92] H. Warita, T. Hayashi, T. Murakami, Y. Manabe, K. Abe, Oxidative damage to mitochondrial DNA in spinal motoneurons of transgenic ALS mice, Brain Res. Mol. Brain Res. 89 (1–2) (2001) 147–152.
[93] M. Lee, D. Hyun, P. Jenner, B. Halliwell, Effect of overexpression of wild-type and mutant cu/Zn-superoxide dismutases on oxidative damage and antioxidant defences: relevance to Down's syndrome and familial amyotrophic lateral sclerosis, J. Neurochem. 76 (4) (2001) 957–965.